Mixed BB–IF Predistortion of OFDM Signals in Non-Linear Channels

Paolo Banelli and Giuseppe Baruffa

Abstract—It is well known that power amplifier induced nonlinear distortions produce a signal spectral regrowth at the transmitter output of digital radio communication systems. This effect is responsible for both adjacent channel interference and BER degradation. Signal predistortion is a technique that counteracts such phenomena. Technological advances in the last decade, renewing the interest in this technique, led to the realization of digital baseband (BB) predistorters that overcome the performance of the existing analog IF (Intermediate Frequency) ones. However, the substitution of an analog IF predistorter with a digital BB one forces to partially redesign the system architecture. An alternative approach is proposed in this paper, based on digital and analog techniques, which combines the precision of the digital BB solution with the practicality of an IF architecture. This solution is particularly interesting to substitute an old analog IF predistorter simply plugging-in the new digital one, without further changes in the transmitter architecture. Critical aspects, predistortion algorithms and simulation performance are presented with respect to a Digital Video Broadcasting system which is based on an OFDM modulation and is very sensitive to nonlinear distortions because of the adopted multicarrier modulation.

Index Terms—Digital broadcasting, IF predistortion, nonlinearity.

I. INTRODUCTION

THE ADVENT of digital broadcasting techniques for television and radio transmissions started a new era in the field of consumer electronics [1], [2]. Extremely interactive audio and video services will be available to each consumer at an affordable price. The overall quality of the service, however, greatly depends upon the complexity of the transmitter and on the irradiated power; at the same time, a plethora of restrictions and bounds, originated by laws or technical and theoretical constraints, limit the capabilities of the system. Requirements on the emission spectrum mask possibly constitute the most severe ones and proper filtering techniques are adopted to fulfill such demands, in order to avoid unwanted interfering signals from falling into adjacent channels. Filtering is effective only if the transmission channel exhibits an ideal (linear) characteristic, such that the theoretical transmission spectrum shape can be easily envisaged from parameters like modulation type, symbol rate, roll-off coefficient of the shaping filter and so on. Nonetheless, the linearity of a real transmission channel
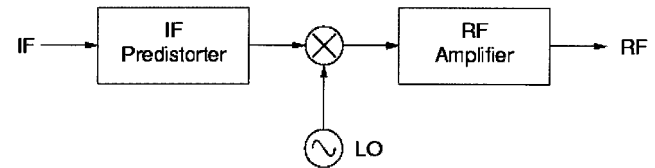
Fig. 1.   Generic architecture of an IF predistortion scheme.

is mostly determined by the final amplification stages at the transmitter side, where devices such as RF power amplifiers are operated in proximity of the saturation point of their input/output characteristics, in order to get an high power efficiency. Since the selected standards adopt multicarrier techniques such as OFDM [3], nonlinearity effects introduce undesired inter-modulation products in the transmitted signal. In the frequency domain, the transmission spectrum is broadened and the inter-modulation noise gives rise to Adjacent Channel Interference (ACI) and in-band interference, the most evident effect of which is an impairment in terms of bit error rate deterioration. The generally adopted solution is to operate the amplifier at a high Input power Back-Off (IBO), i.e., far away from the input saturating point. This choice causes a high Output power Back-Off (OBO), with a consequently reduced dynamic range and power efficiency. This solution can be applied only to Class A amplifiers, that are highly inefficient because their polarization circuit requires a lot of DC power, even if they are characterized by a linear behavior for low input values. It is then preferable a Class AB amplifier, in order to improve the power efficiency at the expenses of linearity. When linearity is required, a different and more efficient approach is to drive the power amplifier with a predistorted signal, which compensates for the nonlinear characteristic of final and intermediate amplification stages. This solution becomes mandatory as the amplifier nonlinearity increases. Several predistortion techniques exist, implemented by means of either a digital or analog processing at the base-band stage [4]. In particular, the digital implementation is generally based upon digital Look-Up Tables (LUTs), combined with a Digital-to-Analog Converter (DAC), that are addressed by the value of the BB undistorted signal [5]. The practical implementation of these systems adopts DSPs or dedicated ASICs in conjunction with ROMs. The digital BB predistortion has some advantages with respect to the digital IF one, such as a reduced working sampling rate. The drawback is that, if BB predistortion is fitted into an already designed system, it usually requires a new arrangement of the bandwidths of the stages ranging from BB up to the IF frequency. In fact, this is done in order to guarantee the required bandwidth to the predistorted signal for an effective
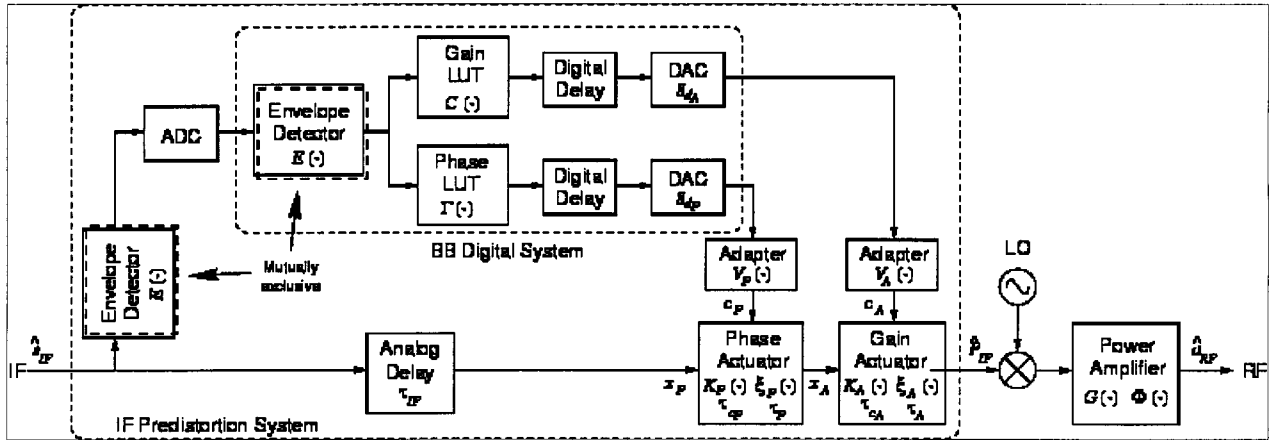
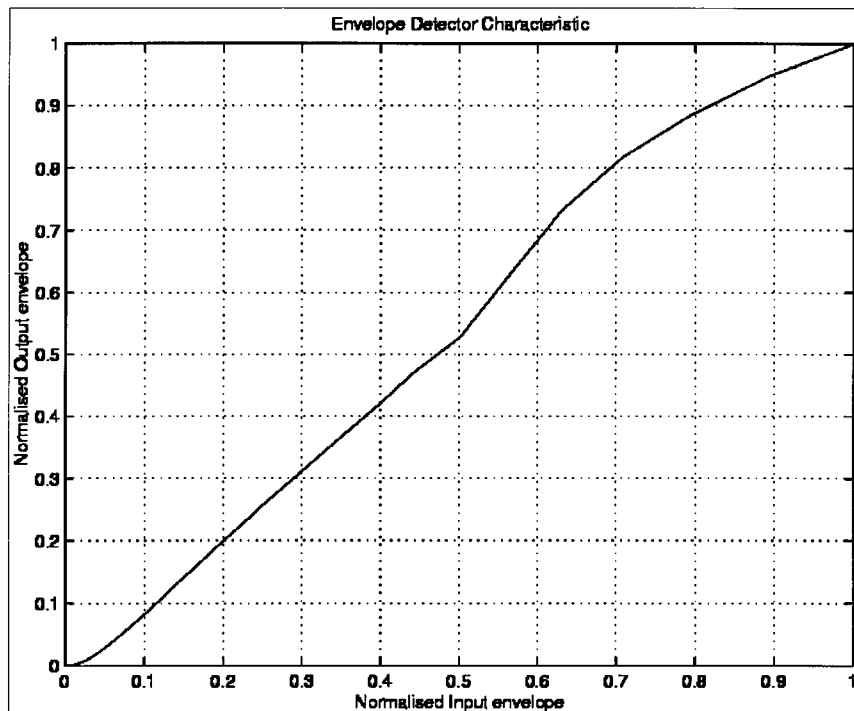Fig. 2.   Implementation scheme of the digital IF predistorter.

Fig. 3.   AM/AM characteristic of the envelope detector adopted in the simulations. Amplitude values are normalized to one.

compensation. Moreover, most existing transmitting systems are equipped by IF analog predistorters [6]. These ones are typically well suited to compensate minor nonlinearities, like those distinctive of Class A amplifiers with small AM/PM distortions. Nevertheless, they are inappropriate for harder nonlinearities, like those distinctive of class AB amplifiers, because of the poor precision granted by the analog components utilized in the implementation of the predistorter. Instead, the adoption of digital techniques at the IF section could allow the amelioration of existing analog techniques, chiefly affording a sharper implementation of the ideal predistortion curves [7]. The implementation of a fully digital predistorter, directly operating on the IF modulated signal, is technologically unfeasible, without a BB down-conversion, for wide band signals like DVB-T, thus redirecting the problem to that of BB predistortion. In this paper we propose a system with a mixed BB–IF architecture, where the BB processing is limited to the

computation of the predistortion, while the predistortion itself is carried out by analog components directly on the IF signal.

II. IF PREDISTORTER ARCHITECTURE

The basic predistortion architecture adopted in this paper is shown in Fig. 1. The IF modulated analog signal is predistorted, then up-converted to RF and eventually fed to the power amplifier. The predistorter is implemented by means of analog and digital components (Fig. 2); the analog IF input is first demodulated by an analog or digital envelope detector in order to evaluate the rms amplitude of the incoming signal. If the analog component is employed, the detector may be represented by its nonlinear AM/AM characteristic, either computed by means of Chebyshev transform in zone zero [8] or evaluated by direct measurement. The result of one measurement for a real device is plotted in Fig. 3. The detected envelope is then digitized at a
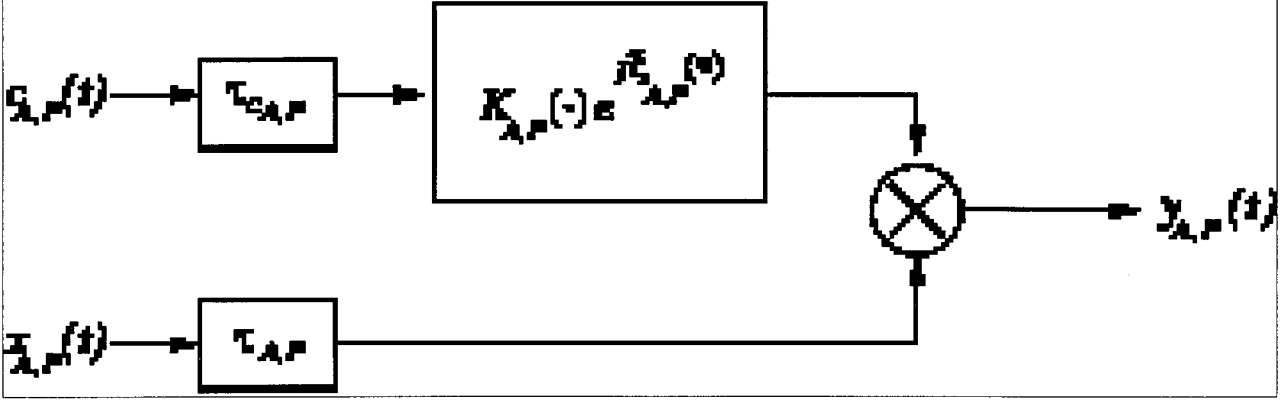
Fig. 4. Generic scheme of an actuator; parameters $\tau_{A,P}$ and $\tau_{cA,P}$ represent time delays of the device.

suitable rate by an Analog to Digital Converter (ADC), or, alternatively, the ADC directly captures the IF signal and a digital envelope detector drives the LUTs containing the predistortion gain and phase curves. The outputs of the LUTs are then digitally delayed to synchronize the control signals to the input signal and converted into analog control streams by two Digital to Analog converters (DACs). Each single control signal is then adjusted in amplitude, in order to supply the correct control voltage to the next actuator. The analog actuators are essentially an AM and a PM modulator; they are driven by the proper control signals to impress the necessary gain and phase correction to the IF signal, such that a linearized characteristic may result by cascading the RF amplifier to the IF predistorter. It is possible to describe the gain and phase actuators with the following general expressions, respectively

$$y_A(t) = x_A(t - \tau_A) K_A \left[c_A \left(t - \tau_{c_A} \right) \right] e^{j \xi_A [c_A(t - \tau_{c_A})]} \quad \text{(1a)}$$

$$y_P(t) = x_P(t - \tau_P) K_P \left[c_P \left(t - \tau_{c_P} \right) \right] e^{j \xi_P [c_P(t - \tau_{c_P})]}, \quad \text{(1b)}$$

where

$x_{A,P}(t)$ are the inputs;

$y_{A,P}(t)$ are the outputs;

$c_{A,P}(t)$ are the control signals (Fig. 4).

The nonideality of the actuator is represented by the functions $K_{A,P}(\cdot)$ and $\xi_{A,P}(\cdot)$ that effect gain and phase variations, and the parameters $\tau_{A,P}$ and $\tau_{cA,P}$ stand for time delays in the device input and control lines, respectively. Fig. 5 shows a comparison between the expected (i.e., ideal) and real behavior of the actuators characteristic obtained by measurement of real AM and PM modulators realized by ITELCO. It is easy to understand that for an ideal gain actuator $\tau_{cA} = \tau_A$, $K_A(c_A) = c_A \cdot g_A + K_{A0}$ and $\xi_A(c_A) = \xi_{A0}$, while for an ideal phase actuator $\tau_{cP} = \tau_P$, $K_P(c_P) = K_{P0}$ and $\xi_P(c_P) = c_P \cdot \phi_A + \xi_{P0}$. A model derived from the Saleh's one [9] has been chosen to represent the nonlinear characteristics of a Class AB amplifier. The nonlinear characteristics can be approximated by the expressions

$$G(\rho) = \frac{a_1 (\rho + \rho_{\text{off}})^2}{b_1 \rho^3} - a_1 \rho_{\text{off}}^2 \quad \text{(2a)}$$
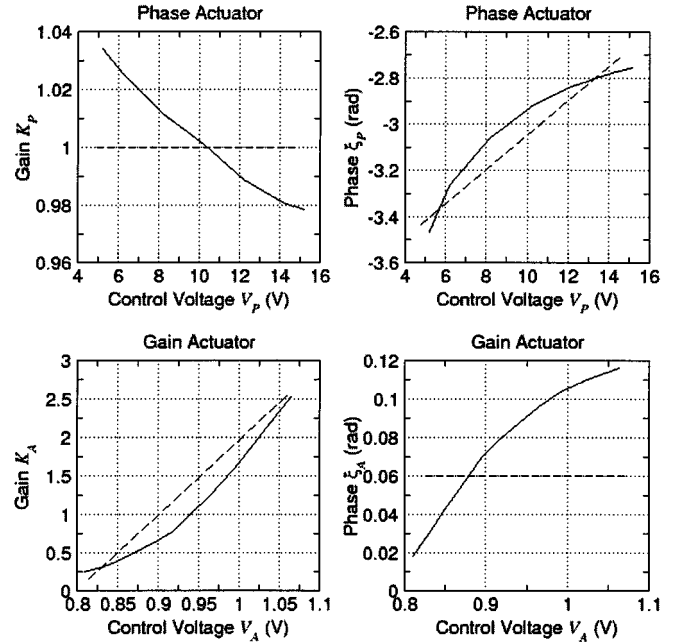
$$\Phi(\rho) = \frac{a_2 \rho^2}{1 + b_2 \rho^2}, \quad \text{(2b)}$$

Fig. 5. Control characteristics for real gain and phase actuators (solid line), compared to the ideal ones (dashed line).

where

ρ	is the input envelope;
$G(\rho)$	is the AM/AM;
$\Phi(\rho)$	is the AM/PM;
ρ_{off}	determines the decay in the AM/AM curve for low values of the input envelope;
a_1, a_2, b_1, b_2	are analog to the coefficients of the Saleh's model.

The expression for $G(\rho)$, which resembles the one in the original Saleh's model, has been chosen such way that its first derivative tends to zero for low input voltage, in order to model the Class AB operation, that is characterized by a concavity of the AM/AM curve for low input voltage. In Fig. 6 the characteristics of the amplifier are plotted for several values of the offset envelope ρ_{off}.

III. COMPUTATION OF THE PREDISTORTION TABLES

The complex envelope of the input IF signal may be denoted by $\hat{s}_{\text{IF}}(t) = A(t) e^{j \theta(t)}$, where $A(t)$ is the instantaneous
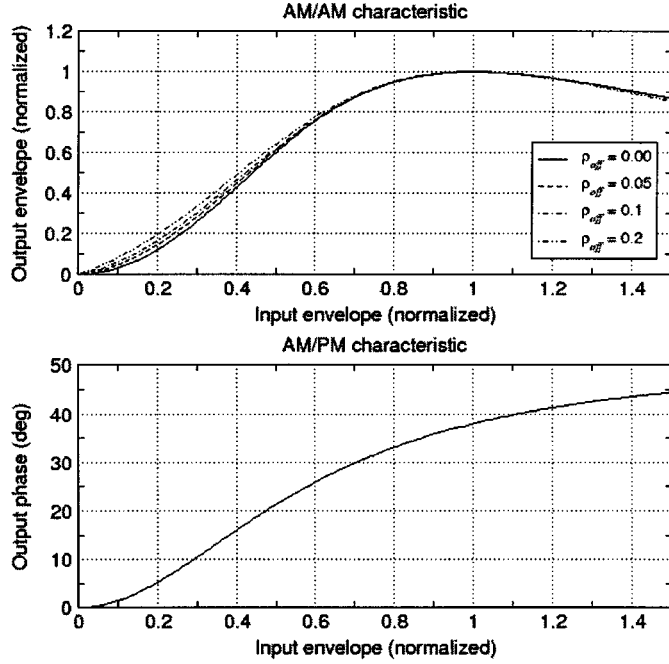
Fig. 6.   AM/AM and AM/PM characteristics of a class AB amplifier with $a_1 = 1.96$, $b_1 = 0.99$, $a_2 = 2.53$ and $b_2 = 2.82$, plotted for several values of ρ_{off}.

envelope and $\theta(t)$ is the instantaneous phase. The predistortion control signals are then expressed by

$$\zeta(a) = c_A(a) = V_A[g_{d_A}C(a)] \tag{3a}$$

$$\psi(a) = c_P(a) = V_P[g_{d_P}\Gamma(a)], \tag{3b}$$

where

$a = E(A)$ is the envelope of the input signal as detected by the envelope detector AM/AM;

$E(\cdot)$, $C(\cdot)$, and $\Gamma(\cdot)$ are the addressable LUT contents;

g_{dA} and g_{dP} are the DAC gains;

$V_A(\cdot)$ and $V_P(\cdot)$ are the gain and phase control voltage adapter characteristics;

The signals $\zeta(a)$ and $\psi(a)$ are, respectively, the gain and phase actuator control signals c_A and c_P.

According to (1a) and (1b) and looking at Fig. 2, the complex envelope of the predistorted IF signal may be expressed as

$$\hat{P}_{\text{IF}} = \left|\hat{P}_{\text{IF}}\right| e^{j \, \arg \hat{P}_{\text{IF}}}$$
$$= AK_P\{V_P[g_{d_P}\Gamma(a)]\}\, K_A\{V_A[g_{d_A}C(a)]\}$$
$$\cdot\, e^{j\theta + j\xi_P\{V_P[g_{d_P}\Gamma(a)]\} + j\xi_A\{V_A[g_{d_A}C(a)]\}}. \tag{4}$$

After the distortion by the nonlinear amplifier, the RF signal complex envelope becomes

$$\hat{a}_{\text{RF}} = G\left\{\left|\hat{P}_{\text{IF}}\right|\right\} e^{j \, \arg \hat{P}_{\text{IF}} + j\Phi\{|\hat{P}_{\text{IF}}|\}}$$
$$= G\{AK_P\{V_P[g_{d_P}\Gamma(a)]\}\, K_A\{V_A[g_{d_A}C(a)]\}\}$$
$$\cdot \exp\big(j\theta + j\xi_P\{V_P[g_{d_P}\Gamma(a)]\}$$
$$+ j\xi_A\{V_A[g_{d_A}C(a)]\}$$
$$+ j\Phi\{AK_P\{V_P[g_{d_P}\Gamma(a)]\}$$
$$\cdot\, K_A\{V_A[g_{d_A}C(a)]\}\}\big). \tag{5}$$

The previous nonlinear expression has to be solved in order to find the values loaded in the predistortion LUTs; it can be accomplished by setting $\hat{a}_{\text{RF}} = k \cdot \hat{s}_{\text{IF}}e^{j\theta_o}$, i.e., the output signal must be a scaled and time-shifted replica of the input one, at least within the amplifier effective operational range. The following conditions are required on the modulus and the phase of $\hat{a}_{\text{RF}}$ in (5):

$$G\{AK_P\{V_P[g_{d_P}\Gamma(a)]\}\, K_A\{V_A[g_{d_A}C(a)]\}\} = kA \tag{6a}$$

$$\theta + \xi_P\{V_P[g_{d_P}\Gamma(a)]\} + \xi_A\{V_A[g_{d_A}C(a)]\}$$
$$+ \phi\{AK_P\{V_P[g_{d_P}\Gamma(a)]\}\, K_A\{V_A[g_{d_A}C(a)]\}\} = \theta + \theta_0. \tag{6b}$$

After some manipulations, it is easy to find the following expressions

$$\zeta(a) = K_A^{-1}\left\{\frac{G^{-1}(kE^{-1}(a))}{AK_P[\psi(a)]}\right\} = f[\psi(a)] \tag{7a}$$

$$\psi(a) = \xi_P^{-1}\{\theta_0 - \xi_A[\zeta(a)] - \phi[G^{-1}(kE^{-1}(a))]\} = h[\zeta(a)], \tag{7b}$$

where $a = E(A)$ is the LUT input, $\zeta(a) = V_A[g_{d_A}C(a)]$ and $\psi(a) = V_P[g_{d_P}\Gamma(a)]$ are the corresponding control signals at the actuator input. (7a) and (7b) are mutually related; they can also be separated to obtain independent expressions as in

$$\zeta(a) = K_A^{-1}\left\{\frac{G^{-1}(kE^{-1}(a))}{AK_P\{\xi_P^{-1}\{\theta_0 - \xi_A[\zeta(a)] - \phi[G^{-1}(kE^{-1}(a))]\}\}}\right\} \tag{8a}$$

$$\psi(a) = \xi_P^{-1}\left\{\theta_0 - \xi_A\left\{K_A^{-1}\left\{\frac{G^{-1}(kE^{-1}(a))}{E^{-1}(a)K_P[\psi(a)]}\right\}\right\}\right.$$
$$\left. - \phi[G^{-1}(kE^{-1}(a))]\right\}. \tag{8b}$$

It must be outlined that $\psi(a)$ and $\zeta(a)$ are the functions used to control the actuators, while the actual functions to be stored on the LUTs are different, because they are fed to the voltage adapters. They may be assumed as linear devices within an operational voltage range, i.e.,

$$\zeta(a) = m_A g_{d_A}C(a) + V_{A_0} \tag{9a}$$

$$\psi(a) = m_P g_{d_P}\Gamma(a) + V_{P_0}, \tag{9b}$$

where m_A, m_P, V_{Ao}, V_{Po} are the linearity coefficients of the adapter characteristics. The entries of the LUTs are then computed as follows

$$C(a) = (\zeta(a) - V_{A_0})/m_A g_{d_A} \tag{10a}$$

$$\Gamma(a) = (\psi(a) - V_{P_0})/m_P g_{d_P}. \tag{10b}$$

Equations (7) or (8) cannot be solved exactly, but an optimal solution is found considering that the predistorting functions are sampled and written in the LUTs. A simple iterative method is shown in Fig. 7; the detected envelope is sampled and it is used to compute ζ_i^j and ψ_i^j, that represent the value of the target functions corresponding to an input value of a_i for the jth step of the iteration. The first LUT value is found by setting $\psi_0^0 = 0$; this is
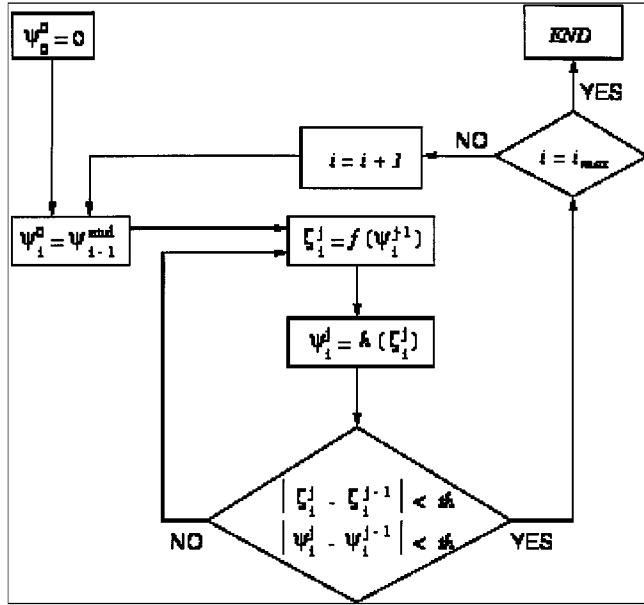
Fig. 7. Iterative method for the solution of (7). For the ith entry of the LUT, ψ_i^0 and ζ_i^0 are the starting values, while ψ_i^{end} and ζ_i^{end} are the final values. The LUTs are sampled into $i_{\max}$ entries.
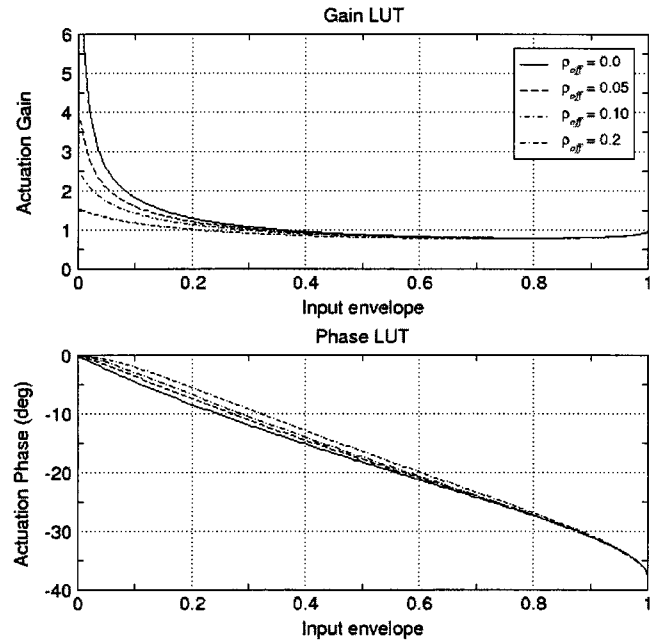

Fig. 8. Predistorter LUTs plotted as control gain and phase versus input detected envelope.

Fig. 9. Gain of the gain actuator versus input envelope. As ρ_{off} increases the gain dynamic decreases.

a correct assumption, since it implies that the AM/PM of the amplifier is zero for a null envelope. At each iteration, new values of ζ_i^j and ψ_i^j are computed by means of the functions $f(\cdot)$ and $h(\cdot)$, by recursively substituting (7a) in (7b) and vice versa. For a single LUT entry, the iteration is stopped either when the absolute difference between consecutive estimated values is below a pre-determined threshold or when a maximum number of cycles has been run. In general, if the amplifier and actuator curves are monotone functions of the control voltage, this algorithm quickly converges to the approximated and sampled solution of (7) and (8) (see the Appendix). If the actuators and the envelope detector were ideal, that means perfectly linear, distortionless and with each actuator controlled by a voltage exactly corresponding to the gain (or the phase) it should apply, (7) become

$$\zeta(a) = G^{-1(A)}/A \qquad (11a)$$
$$\psi(a) = -\phi[G^{-1}(A)], \qquad (11b)$$

which are the classic expressions for a gain based BB predistorter.

IV. RESULTS

Fig. 8 shows a set of predistorter LUT curves computed for the values of the amplifier parameter ρ_{off} shown in Fig. 6, assuming that an ideal detection of the input envelope has been performed. The values are plotted in terms of the effective gain and phase to be applied, as stated in (11). It is evident that the gain dynamic tends to be higher as the parameter ρ_{off} decreases to zero, because of the compression on the output signal for low input envelope values, when ρ_{off} is little. This is critical for a proper correction of the IF signal, since the gain dynamic of the actuator has to be higher than that of the control signal, in order to withstand the AM/AM characteristic. In effect, the absolute values of the gain (both the minimum and the maximum

ones) do not limit at all the predistortion scheme; the presence of further amplification stages between the predistorter and the amplifier can expand the dynamic range of the actuator, while the gain max-to-min ratio remains unchanged. From Fig. 5 the gain actuator gain dynamic is

$$D_{K_A} = \frac{K_{A_{\max}}}{K_{A_{\min}}} \approx \frac{2.537}{0.2646} \approx 9.59 \approx 10 \, \mathrm{dB}; \qquad (12)$$

this value has to be compared with the actuation gain dynamic reported in Fig. 9, computed as the ratio between the generic gain actuation curve and the respective minimum gain. As the
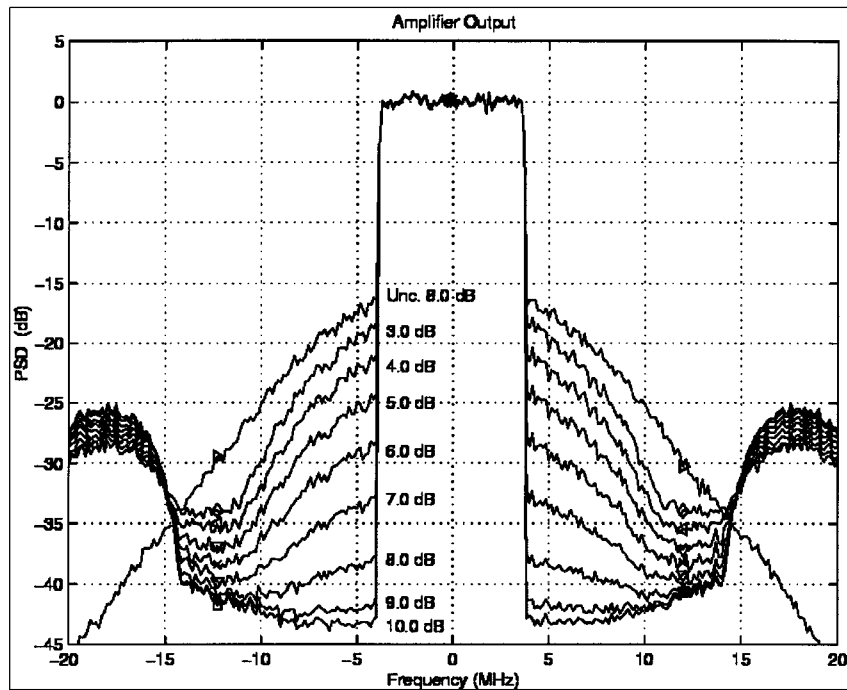
Fig. 10. Spectrum at the amplifier output for the IF precorrector. OBO values range from 3.0 dB to 10.0 dB. The spectra are compared with the one obtained without precorrection at 8 dB OBO. The amplifier has $\rho_{\mathrm{off}} = 0.0$, the precorrector sampling frequency is 36.54 MHz and 10 bit LUTs are used.

parameter ρ_{off} decreases, the required actuation gain dynamic increases and it can be seen that only the curve with $\rho_{\mathrm{off}} = 0.0$ is not fully correctable. However, this side effect has a minor importance over the global behavior of the system, since the correction capability fails only for little envelope values, where the AM/AM curve derivative tends to zero and the predistortion gain tends to be large. For example, when $\rho_{\mathrm{off}} = 0.0$ and for a 1024 entries LUT, only the first six predistortion levels are not defined. A major constraint exists for the phase actuator, because the phase dynamic of the PM modulator can be by no way enlarged after the predistortion stage. The performance of the IF predistortion system has been simulated for the case of a DVB-T signal. It is an OFDM signal, characterized by a large dynamic range and a flat spectrum over the signal bandwidth of 7.6 MHz. The selected transmission mode is the 8k one (8192 carriers) with a circular prefix duration of 1/32nd of the useful OFDM block time and a 16-QAM mapping of the data on the sub-carriers [1]. Due to the coexistence of many digital and analog broadcast signals in the whole service bandwidth (for example, bands IV and V, i.e., 470–860 MHz), spectrum emission templates have been determined in order to avoid that interfering signals occupy adjacent channels. If a proper filtering chain is adopted, nonlinear effects are the primary cause of spectral regrowth outside the channel bandwidth; for example, one of the requirements is that the spectrum level at a frequency offset of 4.2 MHz from the center frequency (i.e., spectrum shoulder) is at least 36 dB lower than the center spectrum level. The obtained performance in terms of shoulder attenuation is depicted in Fig. 10, where the spectrum at the amplifier output is plotted for different values of the OBO. The precorrector adopts a 1024 entries LUT (10 bits of quantization) and operates at a sampling frequency of 36.54 MHz (four times the sample frequency of

the DVB-T signal). The amplifier selected for the simulations has an AM/AM curve with $\rho_{\mathrm{off}} = 0.0$ and the spectra are compared to the one obtained without precorrection, at 8 dB OBO. In this case, for example, the required attenuation of 36 dB is obtained for OBOs larger than 7 dB. This one and the following results are simulated for the same input sequence of 20 DVB-T OFDM blocks, such way that a better comparison among the spectra can be effected. For comparison purposes, simulation results are reported for a BB gain-phase predistorter operating in a configuration similar to that of the IF one, that is with the same number of 10 quantization bits and at the same sampling frequency of 36.54 MHz. Fig. 11 shows output precorrected spectra for different values of the OBO, together with a not precorrected output spectrum. It is evident that the BB predistorter has a larger shoulder attenuation, especially at higher OBOs, because there are neither analog actuators nor analog envelope detectors and it operates on the interpolated digital BB signal. In Fig. 12 the amplifier output spectra are plotted for an OBO of 8 dB and the effects of wrong synchronization between the IF predistorter and the analog input signal are shown. It can be seen that when the synchronization error exceeds 1/32nd of the DVB-T sample time ($T_s = 109$ ns), the spectral regrowth almost vanishes the effects of the predistorter and raises the shoulder level over the threshold level. Again, these results are compared with the spectrum of the not-precorrected signal, at 8 dB OBO. A set of simulations has been run in order to show the effect of the parameter ρ_{off} on the precorrected signal (Fig. 13). As expected, $\rho_{\mathrm{off}} = 0.0$ causes the smallest shoulder attenuation due to the compression of the AM/AM curve for little envelope values, whereas for a greater ρ_{off} the shoulders asymptotically converge to a limit value. On the contrary, the effects of the variation of ρ_{off} on the not predistorted signal (also shown
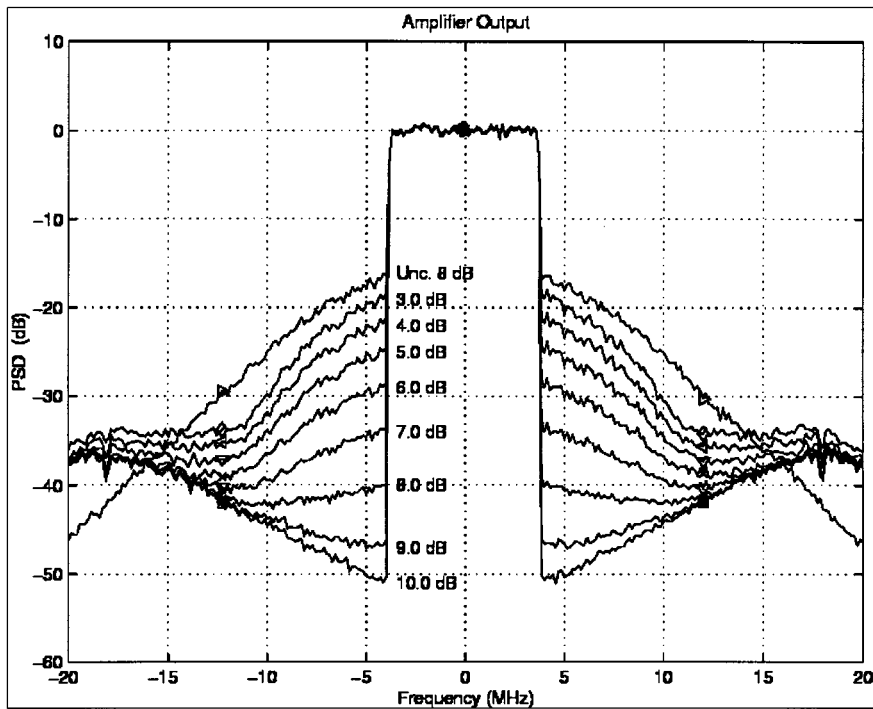
Fig. 11. Spectrum at the amplifier output for a base-band gain-phase precorrector. OBO values range from 3.0 dB to 10.0 dB. The spectra are compared with the one obtained without precorrection at 8 dB OBO. The amplifier has $\rho_{\text{off}} = 0.0$, the precorrector sampling frequency is 36.54 MHz and 10 bit LUTs are used.
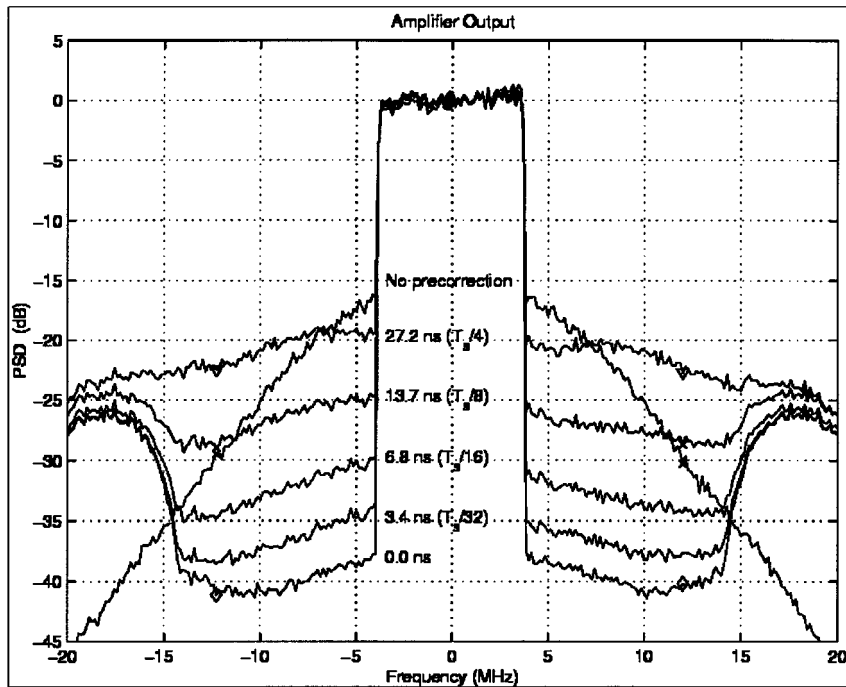

Fig. 12. Spectrum at the amplifier output for 8.0 dB OBO and uncompensated delay between the IF signal and the IF predistortion chain. The delay values are 0.0 ns, 3.4 ns ($T_s/32$), 6.8 ns ($T_s/16$), 13.7 ns ($T_s/8$) and 27.2 ns ($T_s/4$). The spectra are compared to the one obtained without signal precorrection. The amplifier has $\rho_{\text{off}} = 0.0$, the precorrector sampling frequency is 36.54 MHz and 10 bit LUTs are used.

in Fig. 13) are more evident and shoulder attenuation increases proportionally with ρ_{off}. Another parameter that has a great impact on the predistortion system complexity is the sampling frequency of the digital portion of the board: it can range from four (36.54 MHz) to eight times (73.09 MHz) the sample rate of the digital DVB-T stream ($fs = 9.14$ MHz). Fig. 14 shows that,

for a 8 dB OBO, the loss in shoulder attenuation is of about 1 dB when the sampling rate is decreased from 73.09 MHz to 36.54 MHz. The comparison with the spectrum obtained by predistorting the signal with an infinite predistortion bandwidth demonstrates that the loss with respect to the maximum achievable shoulder reduction is slight ($\approx$2 dB). A higher sampling
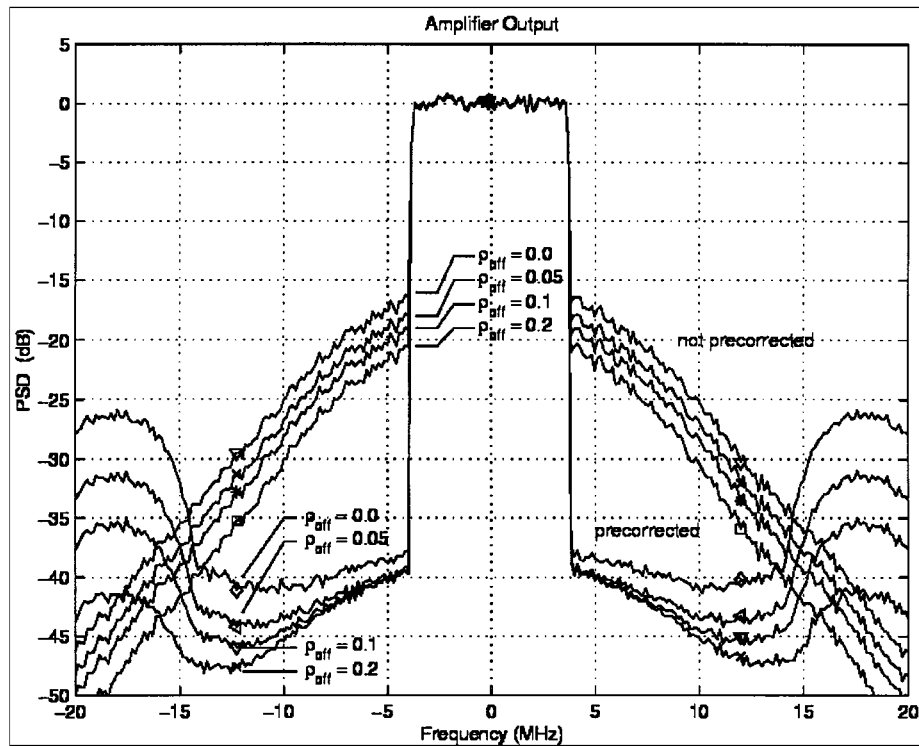
Fig. 13. Spectrum of the IF precorrected and of the not precorrected amplifier output for the parameter ρ_{off} ranging from 0.0 to 0.2. The amplifier OBO is 8 dB, the precorrector sampling frequency is 36.54 MHz and 10 bit LUTs are used.
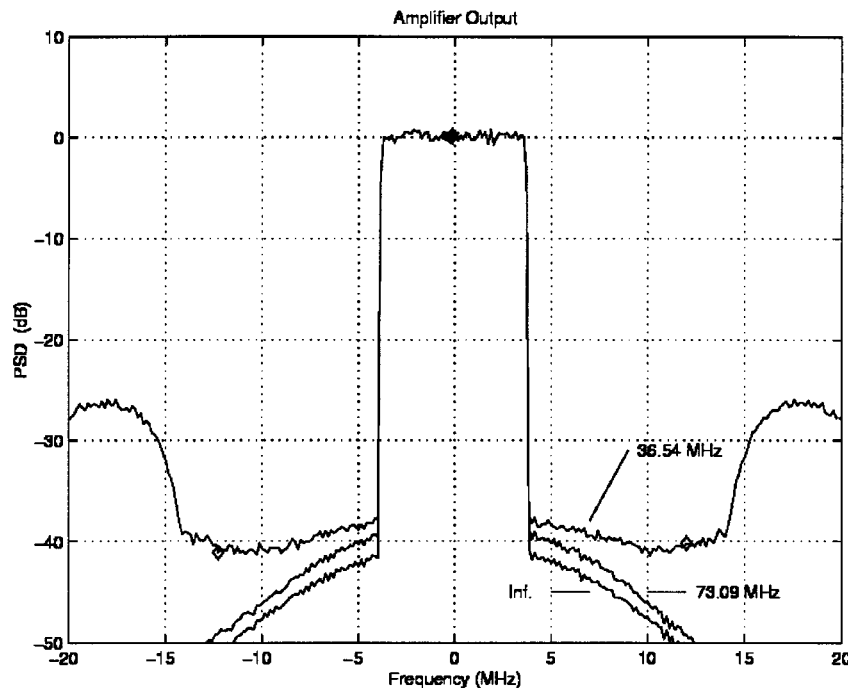

Fig. 14. Spectrum at the amplifier output for 8.0 dB OBO and two different values of the IF precorrector board sampling frequency: 36.54 and 73.09 MHz. The amplifier output spectrum is compared to that obtained by predistorting the signal over an infinite bandwidth. The amplifier has $\rho_{\text{off}} = 0.0$ and the precorrector adopts 10 bit LUTs.

frequency ensures a better operation because the IF precorrector works on the analog envelope signal $\left(\approx\sqrt{x_{re}^2 + x_{im}^2}\right)$, which has a larger bandwidth with respect to in-phase and quadrature base-band components. Correspondingly, control signals with a larger bandwidth feed the actuators, thus allowing an improved

predistortion. This situation is shown in Fig. 15. Such considerations, however, suggest to adopt the lowest sampling frequency for reducing the system complexity and increasing its implementability, at the expense of a little loss in performance. Fig. 16 reports shoulder attenuation at a 4.2 MHz frequency offset from
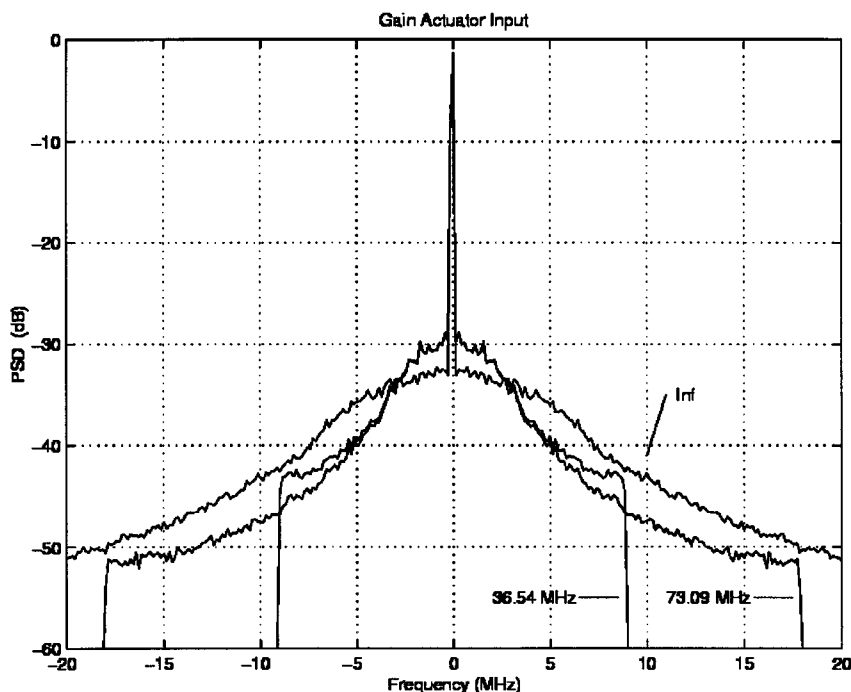
Fig. 15. Spectrum at the gain actuator input for 8.0 dB OBO and two different values of the IF precorrector board sampling frequency: 36.54 and 73.09 MHz. The amplifier output spectrum is compared to that obtained by predistorting the signal over an infinite bandwidth. The amplifier has $\rho_{\mathrm{off}} = 0.0$ and the precorrector adopts 10 bit LUTs.
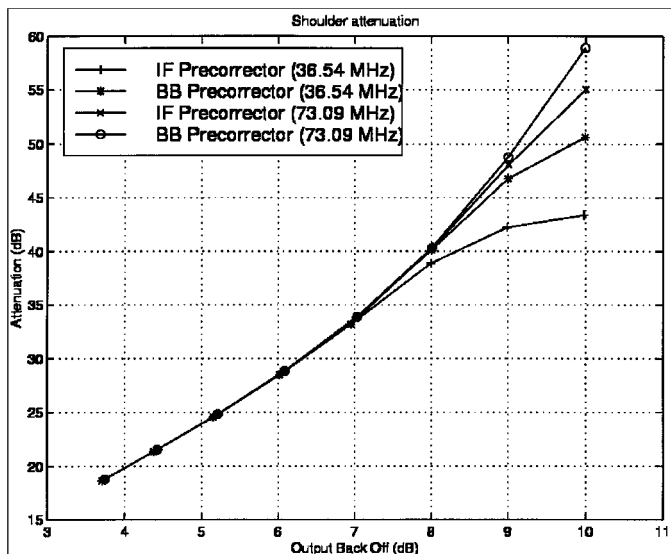

Fig. 16. Shoulder attenuation at a 4.2 MHz offset from center frequency versus Output Back Off, for the IF and the BB gain-phase predistorters. Performance is given at different sampling rates of the IF digital board: four times (36.54 MHz) and eight times (73.09 MHz) the DVB-T sample frequency. The amplifier has $\rho_{\mathrm{off}} = 0.0$ and the predistorter adopts 10 bit LUTs.

the center carrier, for BB and IF predistorters operating at two different sampling rates. As OBO gets larger, the difference between the two techniques becomes evident, as well as the difference with respect to the adoption of a higher sampling rate. However, for an 8 dB OBO, the loss is restricted to just 1 dB, making thus convenient the adoption of an IF precorrector operating at the lower sampling rate. As a final remark, it must be outlined that the system performance is inherently dependent on the amplifier and analog component characteristics. The worst

are the nonlinearities to compensate, the larger is the bandwidth required by the BB processing system for a better predistortion of the IF signal.

V. CONCLUSIONS

In this paper, the possibility to precorrect an IF signal by means of a hybrid digital-analog predistorter has been shown effective. Moreover, a simple algorithm for the computation of the predistortion tables has been introduced, keeping into account both impairments in envelope detection and the non-ideality of actuation devices, too. This technique allows the upgrade of existing analog IF predistortion circuits with only minor or no changes in the architecture of the systems. The selected predistortion method fulfills the requirements of the DVB-T standard in terms of both in-band performance and out-of-band spurious rejection. However, for a proper predistortion of the input signal, an high accuracy in the estimation of delays between the signal line and the predistorter control signal must be reached, by means of precise synchronization. A comparison with a classic BB predistorter has been performed and it shows that the intrinsic loss is little and acceptable. Future work in this area will include a comparison between digital IF and digital BB predistortion techniques in terms of bit error probability, adaptivity and flexibility.

APPENDIX

In order to show the convergence of the iterative method for the computation of the predistortion tables, consider (8). For a given value of a, they are satisfied by generic solutions such that

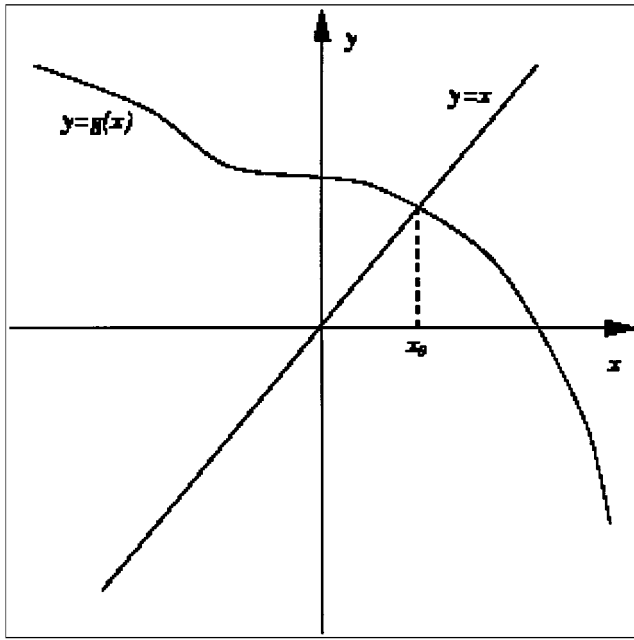$$\zeta_0 = g(\zeta_0) \quad \text{and} \quad \psi_0 = l(\psi_0), \qquad (13)$$

Fig. 17. Graphical representation of the existence of a single fixed point x_o for the equation $x = g(x)$ when the function $g(x)$ is monotonically decreasing.

where ζ_0 and ψ_0 are the fixed points of the functions $g(\cdot)$ and $l(\cdot)$, representing the nonlinear relationships in the right side of the equations. In a simple way, a single fixed point exist if $g(\cdot)$ and $l(\cdot)$ are monotone decreasing functions; for example, functions $y = x$ and $y = g(x)$ cross in only one fixed point x_o if $g(x)$ is monotonically decreasing (see Fig. 17). Denoting by

$$y = \mathrm{MD}(x) \quad \text{and} \quad y = \mathrm{MI}(x), \tag{14}$$

a generic Monotone Decreasing and a generic Monotone Increasing function, respectively, we may evaluate the global behavior of $g(\cdot)$ and $l(\cdot)$. Looking at Fig. 5, it can be seen that

$$
\begin{aligned}
K_P(\cdot) &= \mathrm{MD}(\cdot) \\
\xi_P(\cdot) &= \mathrm{MI}(\cdot) \\
K_A(\cdot) &= \mathrm{MI}(\cdot) \\
\xi_A(\cdot) &= \mathrm{MI}(\cdot).
\end{aligned} \tag{15}
$$

By substituting (15) into (8a), we obtain

$$g(\zeta) = \mathrm{MI}^{-1} \left\{ \frac{T_1}{T_2 \mathrm{MD}\{\mathrm{MI}^{-1}\{T_3 - \mathrm{MI}[\zeta] - T_4\}\}} \right\} \tag{16}$$

where T_1, T_2, T_3 and T_4 are constant values for a determined value of a. According to some simple rules on the composition of continuous monotone functions and considering that the functions of Fig. 5 do not invert sign in their definition domains, it is easy to find that

$$g(\zeta) = \mathrm{MD}(\zeta) \tag{17}$$

and, in a similar way, that

$$l(\psi) = \mathrm{MD}(\psi). \tag{18}$$

Equations (17) and (18) state a sufficient condition for the existence of a single fixed point for each one of (8a) and (8b).

ACKNOWLEDGMENT

REFERENCES

[1] ETSI, EN 300 744—Digital Video Broadcasting (DVB), "Framing structure, channel coding and modulation for digital terrestrial television,", 1.1.2 ed., Aug. 1997.

[2] ETSI, EN 300 401—Radio broadcasting systems, "Digital Audio Broadcasting (DAB) to mobile, portable and fixed receivers,", 2nd ed., May 1997.

[3] W. Y. Zou and Y. Wu, "COFDM: An overview," *IEEE Trans. Broadcast.*, vol. 41, no. 1, pp. 1–8, Mar. 1995.

[4] A. R. Kaye, D. A. George, and M. J. Eric, "Analysis and compensation of bandpass nonlinearity for communications," *IEEE Trans. Commun.*, vol. COM-20, pp. 965–672, Oct. 1972.

[5] M. Faulkner and M. Johansson, "Adaptive linearization using predistortion—Experimental results," *IEEE Trans. Vehicular Technology*, vol. VT-43, no. 2, pp. 323–332, May 1994.

[6] N. Imai, T. Nojima, and T. Murase, "Novel linearizer using balanced circulators and its application to multilevel digital radio systems," *IEEE Trans. Microwave Theory and Techniques*, vol. 37, no. 8, pp. 1237–1243, Aug. 1989.

[7] S. Andreoli, P. Banelli, R. Betti, and E. Fumi, "Sistema di predistorsione misto in banda base ed IF per la linearizzazione di amplificatori," patent no. MC99A000052, Italian Patent Office, Rome, June 1999.

[8] N. M. Blachman, "Detectors, bandpass nonlinearities and their optimization: Inversion of the Chebyshev transform," *IEEE Trans. Inform. Theory*, vol. IT-17, pp. 398–404, July 1971.

[9] A. A. M. Saleh, "Frequency-independent and frequency-dependent nonlinear models of TWT amplifiers," *IEEE Trans. Commun.*, vol. COM-29, pp. 1715–1720, Nov. 1981.